Astronomy & Astrophysics manuscript no. proj1 ©ESO 2019
November 30, 2019

Stellar parameters determination

Project I - Computational Astronomy

Rui Peixoto

Departamento de Física e Astronomia, Faculdade de Ciências, Universidade do Porto

November 30, 2019

ABSTRACT

Aims. A systematic and efficient method to determine stellar parameters from observed spectra by comparison with synthetic spectra is developed and implemented.
Methods. Stellar parameters are estimated and observed spectra are compared with preselected synthetic spectra by equivalent width comparison of select fitted lines. Selected synthetic spectra are then processed and interpolated to facilitate comparison with observed spectra.
Results. Computational method is implemented and two stars analysed. Sensibility to a stars' high rotational velocity, effects of experimental noise, good fit conditions are discussed and pathological cases analysed.

1. Introduction

Spectral analysis is a fundamental tool in astronomy and astrophysics. A good understanding of spectra is a key factor not only to observational astronomy, but also to the understanding of phenomena best displayed in astronomical context, such as high-energy physics, plasma physics and cosmology.

In this context, a systematical analysis of spectra potentiates the value of forthcoming increases in instrumental resolution for accurately determining stellar parameters. The exercise of developing sensible computational methods here employed is therefore a worthwhile endeavor.

2. Spectra Comparison

From the comparison of observed with synthetic spectra one may conclude much about the observed object. While a direct comparison (using a least squares fit method, for example) is possible, it is not the most efficient or insightful approach. To take advantage of refined (and consequently large) synthetic spectra databases, one must explore more efficient ways of comparing spectra. With this goal, we compare instead the equivalent width, W, of known FeI spectral lines (in this case, Tsantaki et al. (2013)).

This method of comparison naturally avoids most of the effects of noise inherent to observed spectra, due to the way of calculating W, while simultaneously providing a considerable speedup.

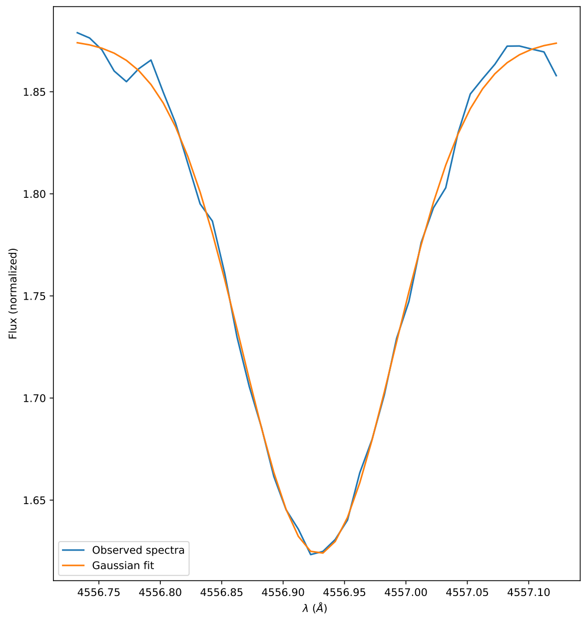

Fig. 1. Gaussian fit to spectral line

3. Method

3.1. Equivalent width and Gaussian fit

At the core of the method is the idea that the equivalent width of a spectral line may be estimated by employing a Gaussian fit (Figure 1) and computing (Monteiro & Gameiro (2019)).

$$W_0 = \int_{\lambda_0-k}^{\lambda_0+k} \frac{F_{\mathrm{cont}} - F_{\mathrm{line}}}{F_{\mathrm{cont}}} \quad (1)$$

where F_{cont} is the continuum line and k some appropriate limitation such that the line is isolated but not cut. Deciding on a good parameter k is in itself a problem that will be discussed in section 4.1. Computationally, the integral need not be computed, as one can get the width from the Gaussian parameters only.

3.2. Temperature estimation

With efficiency in mind, we start by estimating the effective temperature of our spectra, as this allows us to limit the range of

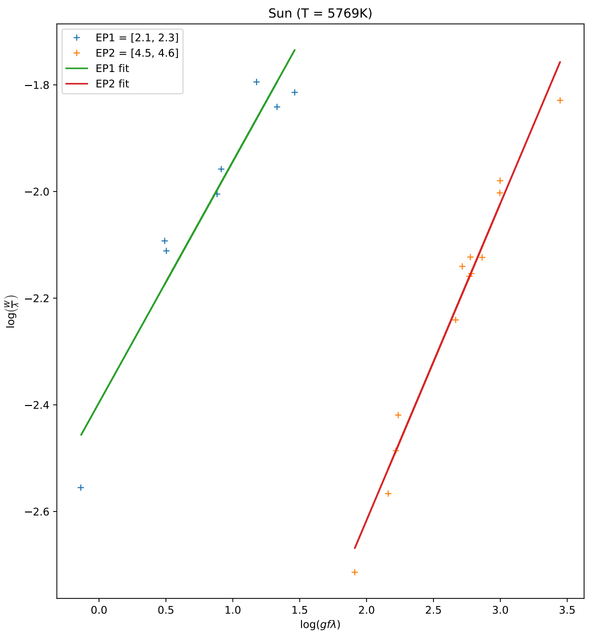

Fig. 2. Sun's temperature estimation

spectra to lookup in the database greatly. We achieve this by calculating the equivalent width of lines of two multiplets of sufficiently different excitation energy and plotting $log\,(W/\lambda)$ by $\log\,(gf\lambda)$. From the relation (Monteiro & Gameiro (2019))

$$\log\left(\frac{W_\lambda}{\lambda}\right) = \alpha + \log\,(\lambda f_i g_i) - \frac{5040}{T_{\rm exc}}\chi_i \tag{2}$$

with $\log\,(\lambda f_i g_i)$ and χ_i know for each multiplet (Tsantaki et al. (2013)), and α a constant, we may denote the average distance between linear fits (for which equation 2 is common) as Δ and obtain

$$T_{\rm exc} = \frac{|5040\,(\chi_2 - \chi_1|)}{\Delta} \tag{3}$$

Using known equivalent widths for the sun's lines (Figure 2) we get $T = 5769$ K directly from equation 3.

3.3. Synthetic spectra database lookup and comparison

Setting an uncertainty interval on the temperature ΔT (in our case, $\Delta T = 400$K), one may now compare the observed spectra with synthetic spectra (in Laverny et al. (2012)) with temperatures in the range $T \in [T - \Delta T, T + \Delta T]$.

This comparison proceeds once again by calculating the equivalent width of known lines of both spectra. We may then plot $W_{\rm synt}$ by $W_{\rm obs}$ and determine the best synthetic spectra by determining the one corresponding to a linear fit of slope closest to unity. [1]

[1] Alternatively, a least squares comparison may be used. The reasons for not using this method will be clarified later. They may nevertheless be reduced to equivalent methods, depending on the choice of lines. Due to the efficiency of computational fitting methods, there is no significant slowdown.

3.4. Synthetic spectra processing

With the best fitting spectra found, one need only process it before the comparison with the observed spectra. This consists of:

1. applying the experimental profile of the instrument of measurement used, by means of a convolution of the spectra with a Gaussian determined by the experimental parameters as in equation 4 (Monteiro & Gameiro (2019)).

$$\sigma = \frac{<\lambda>}{R\sqrt{8\ln(2)}} \tag{4}$$

being σ the standard deviation of the Gaussian function and R the resolution of the instrument ($R \approx 50000$ for HARPS used in Tsantaki et al. (2013)).

2. estimating the rotational velocity of the star $v \sin I$ by Fourier analysis of the spectra and averaging the minima its FFT (see figure 3) over given lines and estimating $v \sin I$ by equation

$$v \sin I = \frac{\Delta\lambda_M}{\lambda_0}c \tag{5}$$

where c is the speed of light, λ_0 the central wavelength of the line, and $\Delta\lambda_M$ obtained by comparison with the values for the Sun, assuming linear limb darkening. Monteiro & Gameiro (2019)

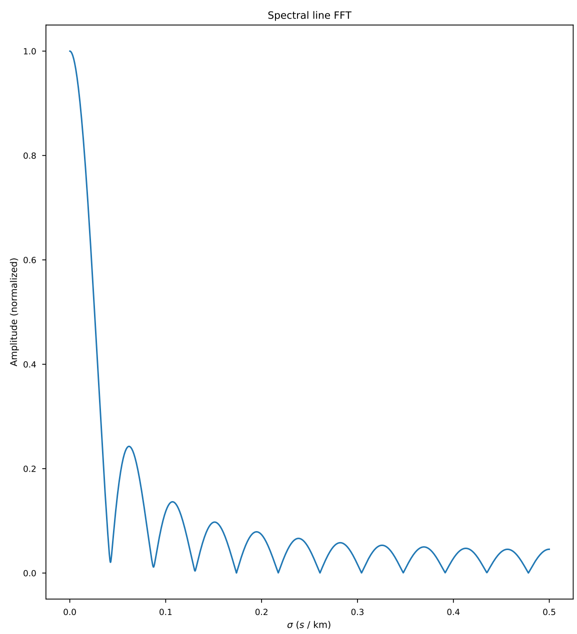

Fig. 3. Spectral line Fourier Transform

3. if rotational velocity is significant, applying a rotational profile to the spectra by convolution with a function of the type in equation 6 (illustrated in figure 4). [2]

$$G_\epsilon\,(\lambda - \lambda_0) = \frac{2(1-\epsilon)\left(1 - \left(\frac{\lambda-\lambda_0}{\Delta\lambda_M}\right)^2\right)^{1/2} + \frac{\pi\epsilon}{2}\left(1 - \left(\frac{\lambda-\lambda_0}{\Delta\lambda_M}\right)^2\right)}{\pi\Delta\lambda_M(1-\epsilon/3)} \tag{6}$$

[2] For our analysis, we estimate ϵ by using it's value for the Sun.

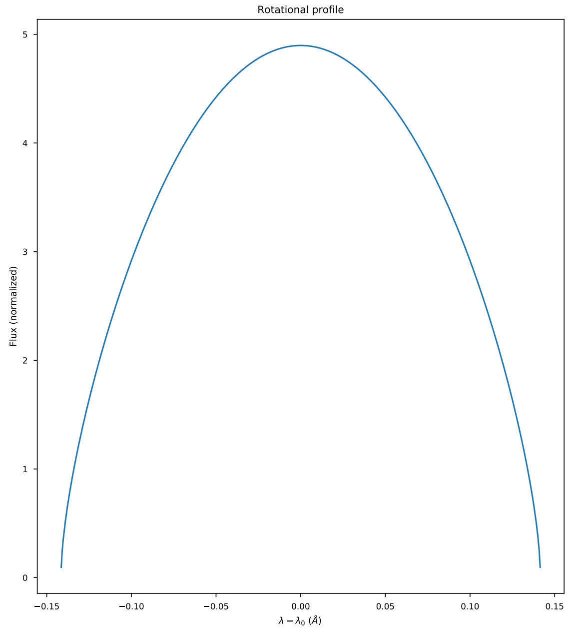

Fig. 4. Rotational profile

4. interpolating the synthetic spectra with observed data for ease of posterior analysis.

4. Fitting pathologies

In some spectra we noted some pathological behavior and conformed our method to avoid it as systematically and consistently as possible. What follows is the analysis of such cases and discussion of the workarounds used.

4.1. Fitting lines - k parameter

While the fitting of lines in observed spectra with fixed k works well, it becomes a problem when calculating equivalent widths of lines in synthetic spectra. In these, multiple lines may get mixed together resulting in the broadening and partial overlapping, as seen in figure 5.

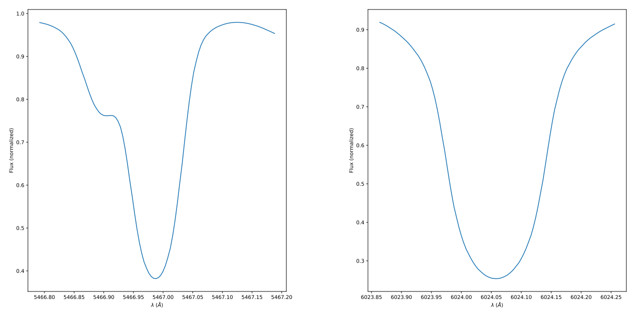

Fig. 5. Behavior of synthetic spectral lines

Here, as efficiency is key, we take advantage of the well-behaved nature of the synthetic spectra and evaluate a step difference function (calculating average difference between points) evaluate the first and second derivative of the function. Our method, however, scales with $O(n)$. that allows us to limit a line to its surrounding maxima, henceforth using the limited line to calculate equivalent widths. The parameter k in equation 1 is therefore automatically determined for these spectra.

The adaptation of this method to the observed spectra is non-trivial because of experimental noise.

4.2. Variable initial conditions in Gaussian fits

The aforementioned behavior of synthetic spectra (or other conditions such as high rotational velocity or turbulence) may induce problems while trying to employ Gaussian fits, with significant line width variation. We handle this by varying the proposed initial conditions for the fit and comparing residuals until we get a good fit.

With effect, this implementation makes it possible to automatically determine the quality of a fit. If no parameters provide a good fit, a line may not behave as a Gaussian (as mentioned in section 4.1), and can be safely ignored.

4.3. Continuum estimation

The main difficulty of our method lies with calculating an accurate estimation of the continuum of the spectra for each line. In general, observed spectra may not be normalized and, because of the characteristics of the instrumentation used, have a different continuum level for different wavelengths.

One can chose from many methods to approach this problem. In the following we discuss the advantages and disadvantages of some of the methods attempted. Additional possible solution are discussed in section 6. [3]

4.3.1. Normalizion with additive Gaussian parameter

If we are adjusting a Gaussian of the form $a \exp\left[\frac{(x-b)^2}{2c^2}\right] + d$ to the line, we may take the additive parameter d as the continuum line and in this manner normalize each line.

This method is vulnerable to the cases where lines are influenced by its neighbors (figure 6).

However, some of this cases may get caught automatically if we refine a tolerance in the estimated quality of the fit sufficiently well.

4.3.2. Normalization by limit estimation

An alternative approach may be to calculate the continuum by averaging the values of the spectra at the line extrema, normalizing the spectra locally before fitting.

This shifts the source of uncertainty in the calculation from the quality of the fit to the estimation of the extrema. If the width of the lines is not predictable along the wavelength range limiting the line properly may be problematic.

[3] This step in our algorithm is purposely left as modular and independent from the rest as possible so different methods may be tried with minimal reformulation of the program.

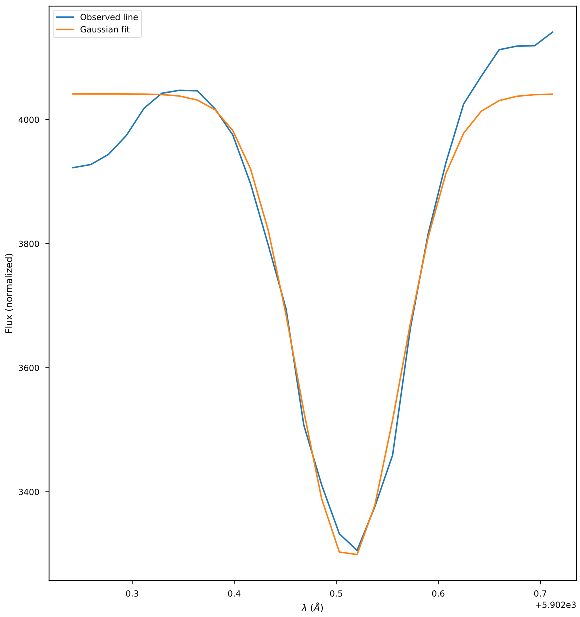

Fig. 6. Pathological case for normalization with additive parameter

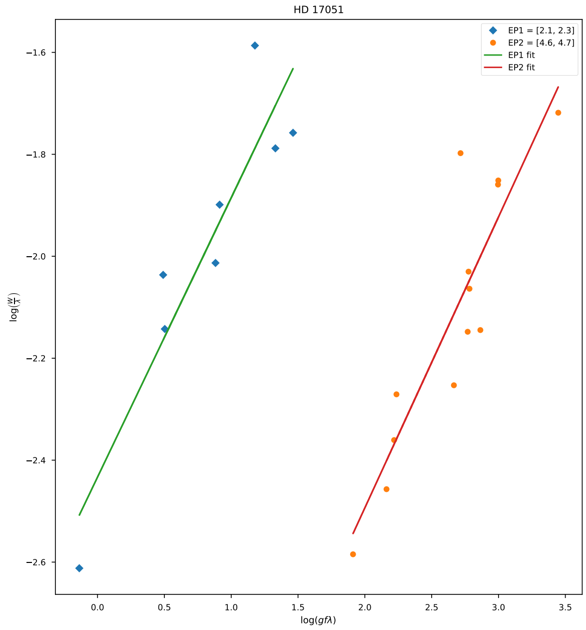

Fig. 7. HD 17051 - $T_{\rm eff}$ estimation

4.4. Multiplet selection

The choice of multiplet used for comparison in temperature estimation (section 3.2) need carefully adhere to the conditions:

1. Both multiplets may be restricted to a small excitation energy range EP1 and EP2.
2. EP1 and EP2 be sufficiently distinct from each other.
3. Lines to be considered in a given multiplet should have similar wavelength.
4. Energy ranges are associated with lines of comparable equivalent widths, so as to enable the computation of average distance between them.

Even under these conditions, better results are obtained from multiplets corresponding to growth curves of similar slope, as seen in figure 2. For keeping under these orientations, a casuistic verification may be needed for optimal results.

4.5. Linear fit method for determining best synthetic spectra

As referenced in section 3.3, the linear fitting method used to compare spectra is generally equivalent to a least squares algorithm. However, that is only true if we are able to compute W of every synthetic line.

In our algorithm, the number of fitted lines may vary from spectra to spectra. As such, employ a linear fitting method, evaluating the difference from unity slope in the plot $W_{\rm synt}$ vs $W_{\rm obs}$, because it is independent of the number of lines fitted.

5. Applications

5.1. Iota Horologii (HD 17051)

The application of our algorithm to HD 17051, a star of low rotational velocity, is immediate, as the observed spectrum used was previously normalized.

We get an estimate of the effective temperature of $T_{\rm eff} = 6085K$, from the growth curves in figure 7. [4]

For this star, all observed lines could be fitted with our algorithm, which found the best fit in our database (Laverny et al. (2012)) listed in table 5.1, compared with measured parameters from Suárez-Andrés et al. (2018).

Parameters	Algorithm	Literature
$T_{\rm eff}$ (K)	6000	6122
$\log g$	4.5	4.37
Z	0.25	0.17
a	0.0	—

Table 1. HD 17051 - stellar parameters

The chosen spectra may also be visually compared (see figure 8). It is clear from visual comparison that not all lines are similar between the spectra. This, of course, is consequence of the coarse parameter space of the database, and of only using some lines for comparison.

5.2. 24 G. Virginis (HD 104304)

We now treat the case of HD 104304, an example of cooler object, with significant rotational velocity.

Like before we estimate the temperature (figure 9) getting $T_{\rm eff} = 5415K$ and the algorithm chooses the spectrum with parameters from table 5.2 (comparison with Aguilera-Gómez et al. (2018)).

The observed spectrum used in this case was not previously normalized, so we see a more significant error from the contin-

[4] The multiplets used do not strictly obey the conditions of listed in section 4.4, in the sense that we use a wide range of wavelengths. This was used because using strictly two simple multiplets as described would provide a small number of equivalent widths to compare. This

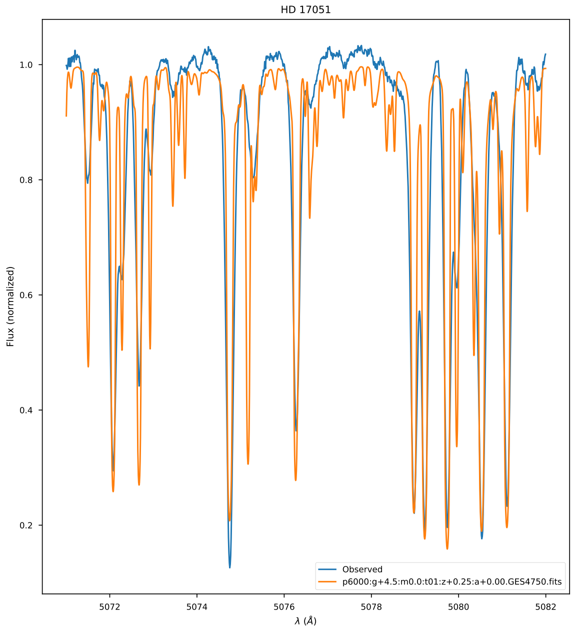

Fig. 8. HD 17051 - Best fitting spectrum

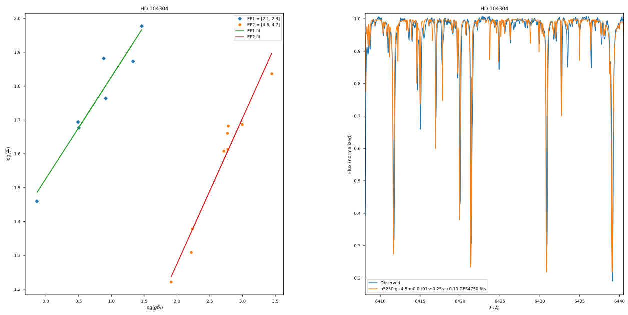

Fig. 9. HD 104304 temperature estimation and spectra comparison

Parameters	Algorithm	Literature
$T_{\rm eff}$ (K)	5250	5506
$\log g$	4.5	4.42
Z	-0.25	0.31
a	0.10	—
$v \sin I$ (kms^{-1})	6.5	5.2

Table 2. HD 104304 - stellar parameters

uum estimation. The broadening of lines caused by the significant rotational velocity also causes this behavior. Our results are therefore a worse estimation of stellar parameters.

is a consequence of the size of our line database. Special attention was used to guarantee that the growth curves behave as expected.

6. Possible improvements

The greatest improvement to this project would come from a refinement of the method used to estimate the local continuum of observed spectra.

One way to go about doing this would be to consider a region around each line, determine the approximate location of all the lines (by computing the second and third derivatives of the spectra, for example), and employing multiple Gaussian fits to the region. This complete information about the line and its neighbors would allow for a much more precise measurement of the continuum value locally.

This method, however, due to the need to estimate line locations (or indirectly, spectra derivatives) is much more sensible to noise, so a noise reduction algorithm would need to be implemented. For this reason, said approach lies beyond the scope of our algorithm, but is used by projects such as ARES (Sousa et al. (2015)).

Our results would also be improved by implementing a wider range of possible functional fits for spectral lines, such as Lorentzian or Voigt profiles. Due to the modular nature of the code, this would be a relatively straightforward implementation.

Application wise, better results would be an immediate consequence of more extensive and parameterically dense line and spectra databases.

7. Conclusions

- An efficient algorithm was developed to determine stellar parameters such as temperature, $\log g$ and metallicity from spectrocospic analysis, by equivalent width comparison.
- The implementation was detailed and different methods discussed.
- Pathological cases were displayed and possible solutions and improvements were discussed.
- An effective application of the algorithm was showed and consequent results discussed.

For more information on the code visit: `https://github.com/ruimpz/spectra`.

Acknowledgements. This work was done under the orientation of professor Jorge Gameiro in the context of the curricular unit of Computational Astronomy.

References

Aguilera-Gómez, C., Ramírez, I., & Chanamé, J. 2018, Astronomy and Astrophysics, 614, A55
Laverny, P. d., Recio-Blanco, A., Worley, C. C., & Plez, B. 2012, Astronomy & Astrophysics, 544, A126
Monteiro, M. J. & Gameiro, J. 2019, Sebenta UC Astronomia Computacional
Sousa, S. G., Santos, N. C., Adibekyan, V., Delgado-Mena, E., & Israelian, G. 2015, Astronomy & Astrophysics, 577, A67
Suárez-Andrés, L., Israelian, G., González Hernández, J. I., et al. 2018, Astronomy and Astrophysics, 614, A84
Tsantaki, M., Sousa, S. G., Adibekyan, V. Z., et al. 2013, Astronomy & Astrophysics, 555, A150